ChemMedChem

Research Article
doi.org/10.1002/cmdc.202300047

Chemistry Europe
European Chemical Societies Publishing

www.chemmedchem.org

Discovery of SI 1/20 and SI 1/22 as Mutual Prodrugs of 5-Fluorouracil and Imidazole-Based Heme Oxygenase 1 Inhibitor with Improved Cytotoxicity in DU145 Prostate Cancer Cells

Loredana Salerno[+],[a] Valeria Sorrenti[+],[a] Valeria Pittalà,[a, b] Valeria Consoli,[a] Maria N. Modica,[a] Giuseppe Romeo,[a] Agostino Marrazzo,[a] Michela Giuliano,[c] Paweł Zajdel,[d] Luca Vanella,[a] and Sebastiano Intagliata*[a]

In this work, we extend the concept of 5-fluorouracil/heme oxygenase 1 (5-FU/HO-1) inhibitor hybrid as an effective strategy for enhancing 5-FU-based anticancer therapies. For this purpose, we designed and synthesized new mutual prodrugs, named SI 1/20 and SI 1/22, in which the two active parent drugs (i.e., 5-FU and an imidazole-based HO-1 inhibitor) were connected through an easily cleavable succinic linker. Experimental hydrolysis rate, and *in silico* ADMET predictions were indicative of good drug-likeness and pharmacokinetic properties. Novel hybrids significantly reduced the viability of prostate DU145 cancer cells compared to the parent compounds 5-FU and HO-1 inhibitor administered alone or in combination. Interestingly, both compounds showed statistically significant lower toxicity, than 5-FU at the same dose, against non-tumorigenic human benign prostatic hyperplasia (BPH-1) cell line. Moreover, the newly synthesized mutual prodrugs inhibited the HO-1 activity both in a cell-free model and *in vitro*, as well as downregulated the HO-1 expression and increased the reactive oxygen species (ROS) levels.

Introduction

Cancer is a global health concern that is considered the leading cause of death in developed countries, accounting for 9.9 million deaths in 2020.[1] The most common cancers in 2020 were breast (2.26 million cases), lung (2.21 million cases), colon (1.93 million cases), and prostate cancers (1.41 million cases); while the most common cause of cancer death was lung cancers (1.80 million deaths).[2] Importantly, the ongoing COVID-19 pandemic had a huge impact on the healthcare system with a decrease in its utilization by about a third during the outbreak.[3] These changes also impacted cancer services by affecting thousands of people which have experienced disruption to their treatments.[4] As a result, medical practices have changed drastically and selected oral-based regimens over intravenous drug-based regimens with comparable efficacy were preferred to reduce the time spent in clinics.[5] Altogether these facts emphasize the need to develop novel anticancer agents with enhanced efficacy and safety profile.

The heme oxygenase (HO) system encompasses two different catalytically active forms of enzymes named HO-1 (the inducible isoform), and HO-2 (the constitutive isoform).[6] These cytoprotective enzymes are primarily localized at the endoplasmic reticulum and are responsible for the heme catabolism generating biliverdin (BVR), bilirubin (BR), carbon monoxide, and ferrous ion as end products.[7] Particularly, in this metabolic pathway, the heme group acts both as a prosthetic group and as a substrate.[8] The HO-1, also identified as heat shock protein 32 (HSP32), is greatly expressed in the liver and spleen. The gene (*HMOX1*) encoding HO-1 is highly induced by stress-related stimuli such as heat shock, ischemia, glutathione depletion, hypoxia, and many other agents generating oxidative stress (i.e., exposure to heavy metals, xenobiotics, and UV irradiation).[9] Of note, HO-1 overexpression has been detected

[a] *L. Salerno,[+] V. Sorrenti,[+] V. Pittalà, V. Consoli, M. N. Modica, G. Romeo, A. Marrazzo, L. Vanella, S. Intagliata*
Department of Drug and Health Sciences
University of Catania
viale A. Doria 6, 95125 Catania (Italy)
E-mail: s.intagliata@unict.it
[b] *V. Pittalà*
Department of Molecular Medicine
College of Medicine and Medical Sciences
Princess Al Jawhara Centre for Molecular Medicine
Arabian Gulf University, Manama 329 (Bahrain)
[c] *M. Giuliano*
Department of Biological,
Chemical and Pharmaceutical Sciences
and Technologies (STEBICEF)
University of Palermo
Via del Vespro 129, 90127,
Palermo (Italy)
[d] *P. Zajdel*
Department of Organic Chemistry
Jagiellonian University Medical College
9 Medyczna Str., 30-688,
Kraków (Poland)
[+] *These authors contributed equally to this work.*

Supporting information for this article is available on the WWW under https://doi.org/10.1002/cmdc.202300047

in several human cancer cells, including prostate, lung, glioblastoma, colorectal, and chronic myeloid leukemia.[10] As a result, high levels of HO-1 in tumor tissues have been correlated to cancer progression, tumor growth, metastasis, and resistance to cancer therapies.[11] In consequence, the pharmacological inhibition of HO-1 emerged as a promising strategy for mono- or adjuvant chemotherapy.[12]

5-Fluorouracil (5-FU) is a fluorinated derivative of pyrimidine antimetabolites, that act by interfering with the metabolic processes within cells (e.g., DNA and RNA synthesis, and cell division).[13] In clinical practice, 5-FU is used in monotherapy and combined therapy to treat a broad set of tumors such as prostate, gastric, colorectal, pancreatic, and breast cancer.[14] Unfortunately, this drug possesses several drawbacks that highly restrict its use including low chemical stability, short plasma half-life, poor bioavailability, and drug resistance phenomenon;[15]; nevertheless, the low tumor selectivity highly affects the overall toxicity to normal cells and tissues. To overcome these problems, various prodrugs of FU, including 5′-deoxy-5-fluorouridine, capecitabine, BOF-A2, ftorafur, UFT, and S-1 have been developed.[16] In addition, several 5-FU-based mutual prodrugs (also known as codrugs) have been designed to improve the biological activity of 5-FU or to achieve its targeted delivery to cancer cells hence reducing the high non-specific toxicity (Figure 1).[17] Among them, the 5-FU/ubenimex codrug (BC-01) showed enhanced *in vitro* and *in vivo* anti-cancer and anti-metastasis effects compared to the parent compounds or their co-administration.[18] Similarly, the Pt(IV)-5-FU hybrid (fuplatin 14) highly increased DNA damage and cell apoptosis with improved cellular accumulation in HCT-116 cancer cells resulting in significant antitumor effect *in vivo*.[19] Also, 5-FU/mitochondria-targeting mutual prodrugs have been developed by conjugating 5-FU and compound F16 to specifically target mitochondria in cancer cells. The resulting hybrid F16-OOC-FU exhibited stronger antiproliferative activity in SGC-7901 cells and lower toxicity towards the GES-1 nontumor cells. With this in mind, we have recently developed the first 5-FU/HO-1inhibitor mutual prodrug (SI 1/17) obtained by connecting the hydroxymethyl-derived 5-FU,[20] with a potent non-competitive HO-1 inhibitor via a succinyl cleavable linker (Figure 1). Interestingly SI 1/17 showed an appropriate chemical and enzymatic stability compatible with its significant anticancer effect in A549 lung cancer cells, as well as reduced cytotoxicity toward a non-tumorigenic lung epithelial cell line.[21]

These encouraging preliminary results, along with our current interest in developing anticancer-based codrugs, prompted us to synthesize two novel 5-FU/HO-1inhibitor mutual prodrugs, named SI 1/20 and SI 1/22 (Figure 2), along with SI 1/17 that has been resynthesized using a new optimized method (Scheme 1). A design strategy involved the replacement of the HO-1 inhibitor counterpart 1-(3-bromophenyl)-2-(1*H*-imidazol-1-yl)ethanol (S1 1/09) with the potent and more selective azole-based analogs 1-(biphenyl-3-yl)-2-(1*H*-imidazol-1-yl)ethanol, and 1-{4-[(4-bromobenzyl)oxy]phenyl}-2-(1*H*-imida-

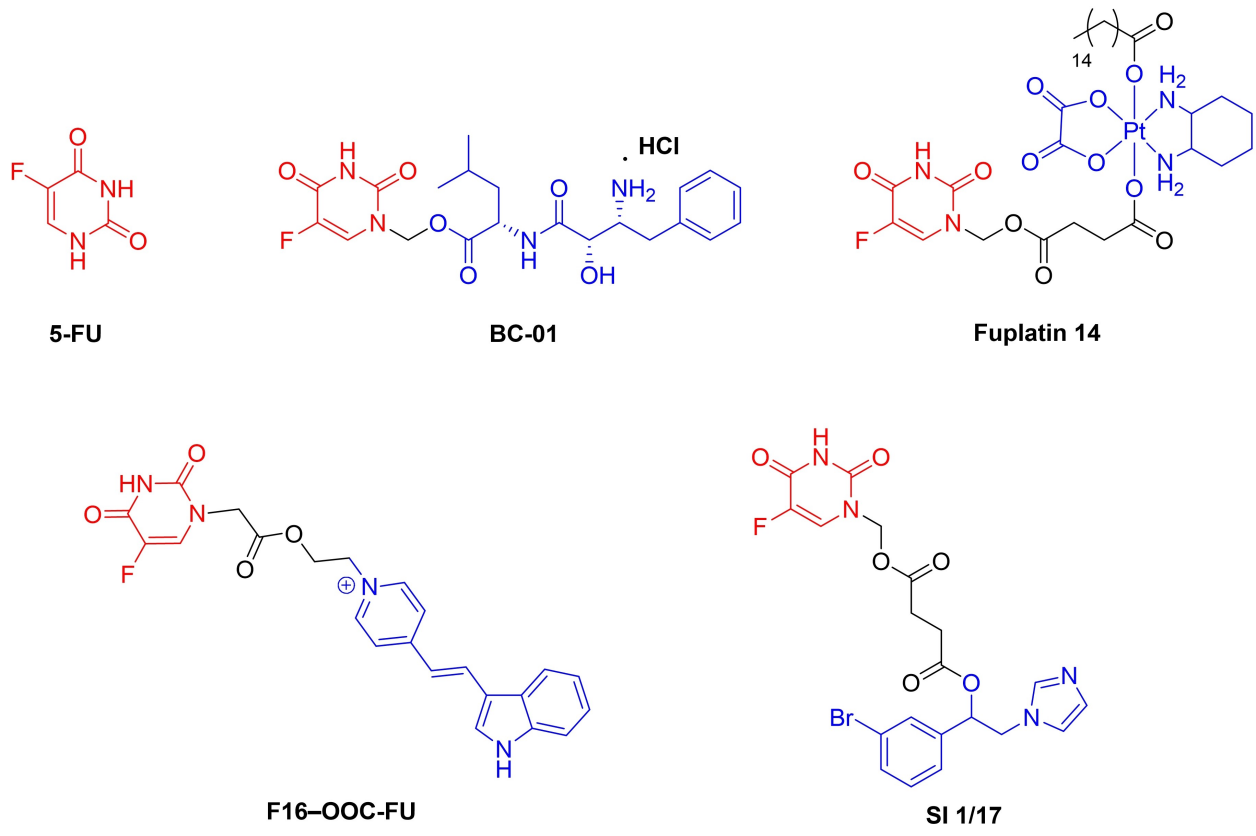

Figure 1. Chemical structure of 5-FU and representative 5-FU-based mutual prodrugs.

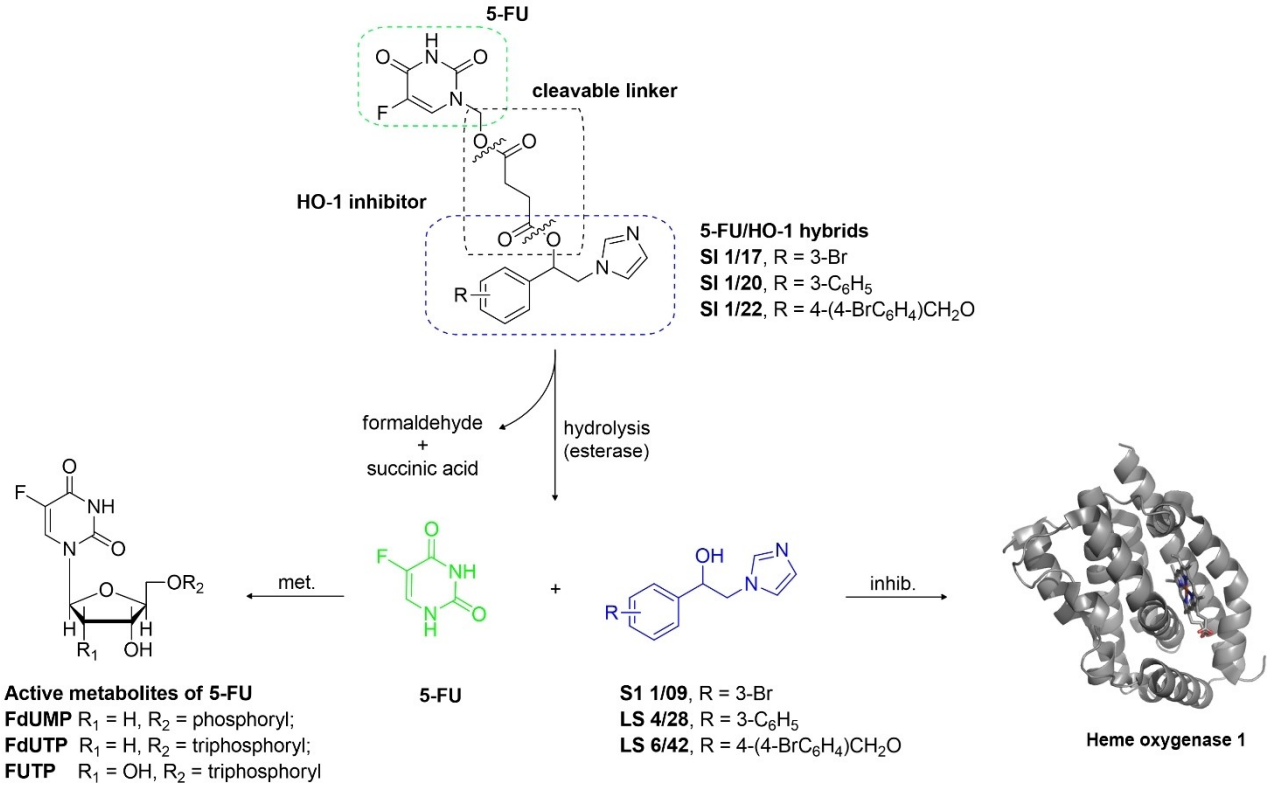

Figure 2. The design strategy of 5-FU/HO-1 inhibitor mutual prodrugs.

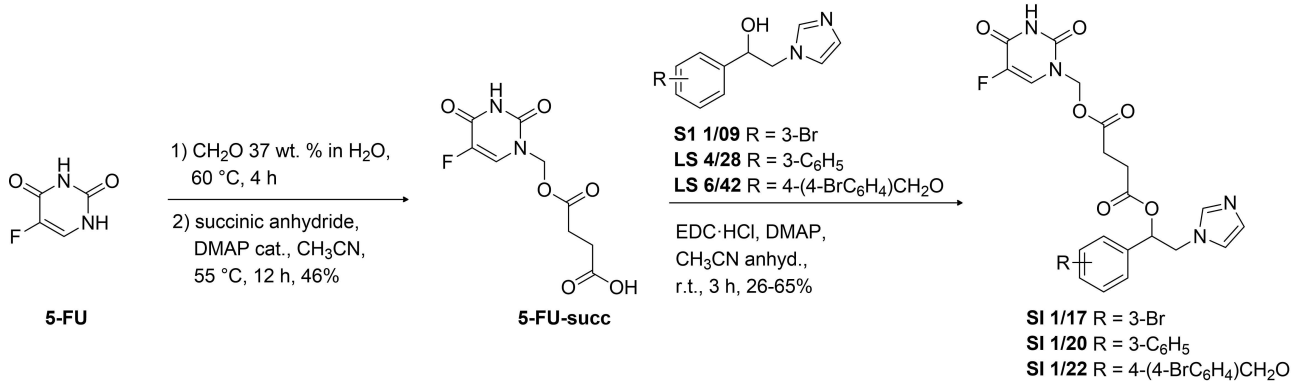

Scheme 1. Reagents and conditions for the synthesis of 5-FU/HO-1 inhibitor mutual prodrugs.

zol-1-yl)ethanol (LS 4/28 and LS 6/42, respectively) previously discovered by our research group (Figure 2).[22] The newly synthesized compounds were then assessed for *in vitro* stability, HO inhibitory activity in spleen/brain microsomal fractions and intact cells, and the *in vitro* antiproliferative effects against lung and prostate tumorigenic cells and prostatic non-tumorigenic cells, respectively.

Results and Discussion

Synthesis of 5-FU/HO-1 inhibitor mutual prodrugs

Here, an optimized and straightforward synthesis of SI 1/17, SI 1/20, and SI 1/22 has been developed and depicted in Scheme 1. SI 1/17 was previously obtained by coupling the key intermediate 4–(1-(3-bromophenyl)-2-(1*H*-imidazol-1-yl)ethoxy)-4-oxobutanoic acid (not shown) with 1-hydroxymethyl-5-fluorouracil, according to a recently described synthetic procedure.[21] However, to increase the yield and easily prepare new hybrid analogs, compounds SI 1/17, SI 1/20, and SI 1/22

were alternately obtained by esterification of 4-[(5-fluoro-2,4-dioxo-1,2,3,4-tetrahydropyrimidin-1-yl)methoxy]-4-oxobutanoic acid (5-FU-succ) with the corresponding arylethanolimidazole derivatives S1 1/09, LS 4/28, and LS 6/42, respectively, using 1-ethyl-3-(3-dimethylaminopropyl)carbodiimide (EDC) hydrochloride as an activating agent, and 4-dimethylaminopyridine (DMAP) as a catalyst. Key precursors (i.e., 5-FU-succ and azole-based derivatives) were prepared following known methods.[19,22] Particularly, 5-FU-succ was prepared by reaction of 5-FU with formaldehyde aqueous solution, followed by treatment with succinic anhydride in the presence of DMAP.

Analysis of the ^{1}H NMR and ^{13}C NMR spectra confirmed the structure of final compounds (Figure S1–S10). Especially, in the ^{1}H NMR spectra, key resonance signals belonging to the 5-FU moiety at δ 8.09 ppm, as a doublet ($J_{H\text{-}F}$ = 6.6 Hz), from the methine proton at the 6-position of the 5-FU ring and around δ 5.59–5.51 ppm, as a multiplet, from methylene protons at the N_1 of 5-FU were observed. In addition, the signal of the methine proton of the phenylethanolic chain gave a characteristic triplet (J = 5.8 Hz) around δ 6 ppm. Finally, signals attributable to the protons of the succinyl spacer were present at δ 2.69 – 2.54 ppm, as a symmetric multiplet. Similarly, key signals belonging to the 5-FU moiety were detected at near 157.4 (d, $J_{C\text{-}F}$ = 26 Hz), 149.2, 139.4 (d, $J_{C\text{-}F}$ = 231 Hz), and 129.4 (d, $J_{C\text{-}F}$ = 34 Hz) ppm in the ^{13}C NMR spectra of all compounds. Finally, aliphatic methine of the phenylethanolic chain was present around δ 74 ppm, while methylenes of the succinyl spacer were present at δ 28.5 and 28.3 ppm.

In vitro enzymatic hydrolysis rate of 5-FU/HO-1 mutual prodrugs and ADMET prediction

According to the mutual prodrug approach, the 5-FU/HO-1 hybrids need to release the active parent drugs, 5-FU and the azole-based HO-1 inhibitors, to exert their biological effects. Therefore, stability studies in aqueous porcine esterase solution and phosphate-buffered saline (PBS) were performed. Data concerning the hydrolysis rate and *in vitro* half-life are reported in Table 1 and Figures S11, and S12 (Supporting Information), respectively. As can be seen from the data, the hydrolysis rate profile for the hybrids in porcine esterase solution fitted with the pseudo-first-order kinetic model, and about 50% of compounds were hydrolyzed by porcine esterase within six hours (*i.e.*, 108 and 335 min, respectively; Table 1). Notably, SI 1/20 resulted stable in PBS solution, while SI 1/22 was readily hydrolyzed in aqueous media. This aspect might be related to the differences in the electron density of the benzene ring concerning either the position or electron effects of its substituents (*i.e.*, 3-phenyl *vs* 4-bromobenzyloxy). Overall, these results suggest that hybrids SI 1/20 and SI 1/22 are likely to be hydrolyzed into parent compounds *in vivo*.

Taking advantage of the nature of SI 1/20, and SI 1/22 as mutual prodrugs the new 5-FU-based hybrids might improve their drug-likeness and pharmacokinetic properties, hence potentially overcoming some of the drawbacks that hinder the clinical use of 5-FU (e.g., short plasma half-life, variable bioavailability, highly non-specific toxicity). Predicted physicochemical properties and *in silico* ADMET parameters of the newly synthesized mutual prodrugs were calculated using the DataWarrior software[23] and the PreADMET web server[24] (Tables 2 and 3, respectively). Consistent with previously reported outcomes obtained for the 3-bromo analog SI 1/17, the new hybrids SI 1/20 and SI 1/22 showed a suitable drug-likeness profile that generally complies with both the Lipinski's rule of five[25] and the MDDR-like rule[26] (Table 2).

The *in silico* ADME results (Table 3) showed a predicted pharmacokinetic profile suitable for their oral bioavailability (HIA > 70% and P_{app} cell permeability > 4), whereas moderate blood-brain barrier penetration (BBB < 2) and strong binding to plasma proteins (PPB > 90%) were predicted. Also, the new hybrids were not predicted to be a substrate of the cytochrome P450 2D6 (CYP2D6), while they might be a substrate of the isoform CYP3A4, most likely due to the presence of an imidazole ring in their structure. However, this possible limitation in their distribution properties might be overcome by loading them into proper nanoparticles formulation that can help a suitable drug delivery of the molecules as well as prevent an early release of parents drugs in plasma. *In vitro* and *in vivo* pharmacokinetic studies are needed to define these new substances. Finally, unlike 5-FU, no serious toxicity, including mutagenic, tumorigenic, irritant, and reproductive effects were predicted for the new mutual prodrugs (Table 3). These potential advantages over 5-FU justify further development of new 5-FU/HO-1 hybrids.

Table 1. *In vitro* enzymatic hydrolysis stability of 5-FU/HO-1 inhibitor mutual prodrugs.

Compd	Porcine esterase[a]		PBS (pH = 7.4)[a]	
	k [min^{-1}]	$t_{1/2}$ [min]	k [min^{-1}]	$t_{1/2}$ [min]
SI 1/20	6.37×10^{-3}	108	0.76×10^{-3}	917
SI 1/22	2.06×10^{-3}	335	1.83×10^{-3}	378

[a] Values from three independent experiments.

Table 2. Predicted physicochemical properties of 5-FU, and 5-FU/HO-1 inhibitor mutual prodrugs.

Compd	Lipinski's rule of five[a]					MDDR-like rule[b]
	MW	cLogP	HBD	HBA	Drug-like	Drug-like
5-FU	130.08	−0.84	2	4	Yes	No
SI 1/20	506.49	2.05	1	10	Yes	Yes
SI 1/22	615.41	2.47	1	11	No	Yes

[a] Molecular weight (MW), calculated LogP (cLogP), number of hydrogen bond donors (HBD), and number of hydrogen bond acceptors (HBA) were predicted using DataWarrior software. [b] MDDR-like rule was predicted using PreADMET web-based application (https://preadmet.webservice.bmdrc.org/): drug-like = No. Rings ≥ 3, No. Rigid bonds ≥ 18, No. Rotatable bonds ≥ 6; nondrug-like = No. Rings ≤ 2; No. Rigid bonds ≤ 17, No. Rotatable bonds ≤ 5; mid-structure = structures of the other ranges.

Table 3. *In silico* ADMET properties of 5-FU and 5-FU/HO-1 inhibitor mutual prodrugs.

Parameter[a]		5-FU	SI 1/20	SI 1/22
Absorption	HIA (%)	75.9	98.2	99.0
	P_{app} (nm/s)	17.3	21.8	24.4
Distribution	PPB (%)	8.3	89.2	88.7
	BBB (C_{brain}/C_{blood})	0.2	0.1	0.1
Metabolism	CYP2D6	none	non-substrate	non-substrate
	CYP3A4	none	substrate	substrate
Toxicity	Mutagenic	high	none	none
	Tumorigenic	high	none	none
	Irritant	high	none	none
	Reproductive	high	none	none

[a] Selected ADME properties were predicted using PreADMET web-based application (https://preadmet.webservice.bmdrc.org/): human intestinal absorption (HIA), range 70–100% = well-absorbed; *in vitro* Caco-2 cell permeability (P_{app}), range 4–70 = middle permeability; *in vitro* plasma protein binding (PPB), > 90 = strong binding; *in vivo* blood-brain barrier penetration (BBB); 2.0–0.1 = permeability to CNS. Selected toxicity properties were predicted using DataWarrior software.[23]

Effects of SI 1/20 and SI 1/22 on cancer cell viability

Firstly, new hybrids SI 1/20 and SI 1/22, were tested in the MTT assay to evaluate their effect on cell viability in lung A549 and prostate DU145 cancer cell lines (Figure 3). These cell lines were selected owing to the documented HO-1 overexpression, which has been demonstrated to contribute to tumor invasiveness.[10] Hybrid compounds showed higher activities than corresponding HO-1 inhibitors in both cell lines, even though the A549 cell line was more sensitive to the treatment with the hybrids compared to DU145 cells (Figure 3A and 3B, respectively). In line with our previous finding, the A549 cell line was also more sensitive to the 5-FU treatment. As a result, no significant differences in 5-FU and hybrids effects (particularly SI 1/20) were observed in this cancer cell line. On the other hand, the 5-FU effect was lower in DU145 cells than in A549 (Figure 3A and 3B), while hybrids showed an improved effect on cell viability at the tested doses compared to the parent drugs. Interestingly, SI 1/22 showed a statistically significant effect in a dose-dependent manner compared to 5-FU (Figure 3B); thus resulting in the most interesting compound.

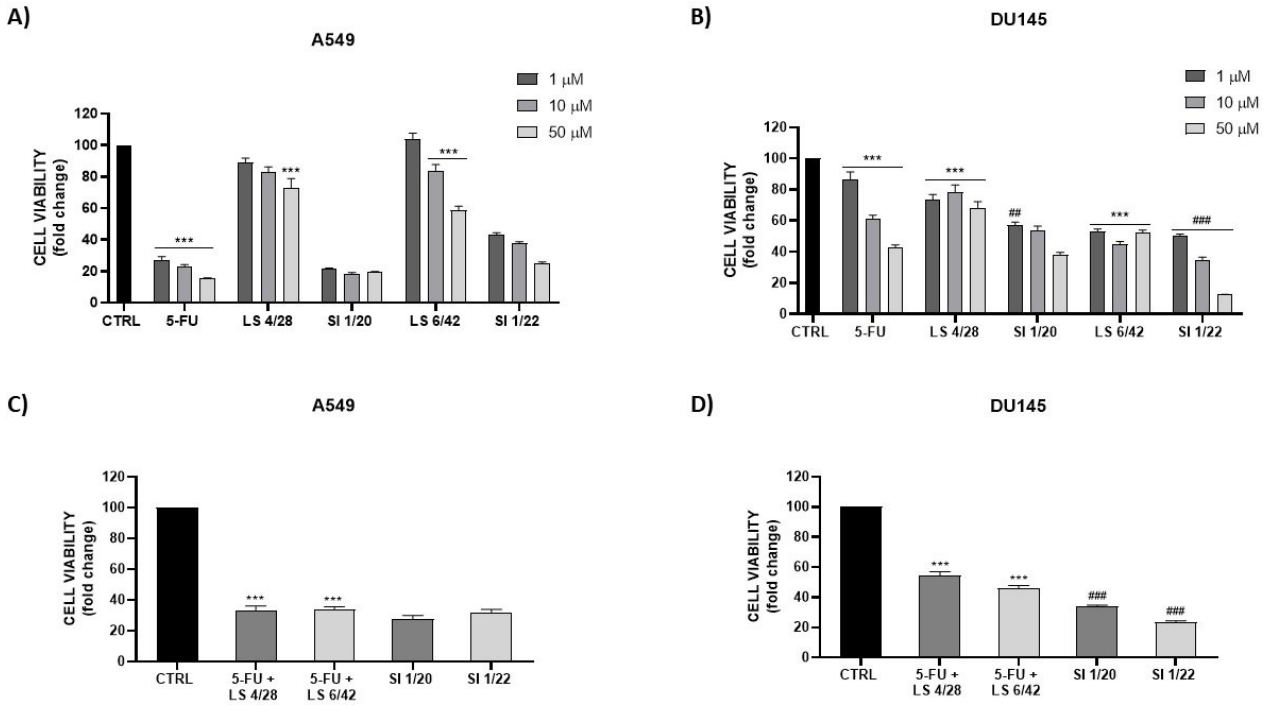

Figure 3. Assessment of 5-FU, LS 4/28, LS 6/42, SI 1/20, and SI 1/22 effects at 1, 10, 50 μM against A549 (**A**) and DU145 (**B**) cell viability after 72 h treatment; effectiveness of co-administration of 5-FU (10 μM) and HO-1 inhibitors LS 4/28, and LS 6/42 (10 μM) compared to mutual prodrugs SI 1/20 and SI 1/22 against A549 (**C**) and DU145 (**D**) cells after 72 h treatment. ***$p < 0.0005$ *vs* untreated control cells (CTRL); ##$p < 0.005$, ###$p < 0.0005$ *vs* 5-FU, 5-FU + LS4/28, 5-FU + LS6/42.

Secondly, to corroborate the possible additive or synergistic effect mediated by the parent drugs, and to determine whether or not the effectiveness of hybrids might be similar or better than the physical mixture, the effect on cells viability for co-administration of 5-FU and HO-1 inhibitors at 10 μM concentration was assessed (Figure 3C and 3D). Of note, both SI 1/20 and SI 1/22 exhibited a significantly higher cytotoxic effect on DU145 cells compared to the combo administration which mimics the physical mixture (i.e., 1:1 ratio of 5-FU and the corresponding HO-1 inhibitor at 10 μM, respectively).

Subsequently, to investigate a desired selective effect of SI 1/20 and SI 1/22 between cancer and normal cells, their cytotoxicity effect has been also tested against selected non-tumor cells such as the human benign prostatic hyperplasia cell line (BPH-1). Notably, both hybrids showed statistically significantly lower cytotoxicity than 5-FU on BPH-1 cells revealing selectivity towards cancer *vs* non-cancer cells (Figure 4). Altogether, these data suggested that the newly synthesized mutual prodrugs exerted improved effects on cancer cell viability compared to parent drugs, supporting the efficacy of our designed approach *in vitro*. According to the above-mentioned data on the hybrids' activity on selected cancer cell lines, SI 1/20 and SI 1/22 were further evaluated using the DU145 cells.

Effect of 5-FU/HO-1 inhibitor mutual prodrugs on HO inhibition in a cell-free model and DU145 cells

The inhibitory activity of the newly synthesized hybrids towards both the HO-1 (rat spleen fraction) and HO-2 (rat brain microsomal fraction) isoforms has been evaluated. Compounds' potency has been expressed as IC_{50} (μM) and the results are reported in the Supporting Information (Table S1). Unsurprisingly, a lower inhibitory potency of the 5-FU/HO-1 inhibitor mutual prodrugs compared to the parent drugs S1 1/09, LS 4/28, and LS 6/42 was observed (205-, 11- and 9-fold, respectively). On the other hand, hybrids SI 1/20 and SI 1/22 had greater potency than SI 1/17 (HO-1 IC_{50} = 10.04 and 8.95 *vs.* 82 μM, respectively). These results were consistent with previous structure-activity relationship studies (SARs) on arylethanolimidazole derivatives corroborating the crucial role of the hydroxyl group in the central ethanolic chain for the modulation of compounds' potency and selectivity towards HO-1, most likely due to an effective hydrogen bond interaction mediated by a consensus water molecule.[27] It should be stressed that as mutual prodrugs, no biological activity for the new compounds is required in their initial chemical form, while the hydrolytic cleavage of the linker leading to the release of the crucial hydroxy group belonging to the parent HO-1 inhibitor is pivotal for enzyme inhibition, therefore the lower potency of hybrids with respect to HO-1 inhibitors is not a limitation.

Concerning the selectivity index (SI), expressed as the HO-2 IC_{50}/HO-1 IC_{50} ratio between the two isoforms, no significant preference was observed (SI = 1.5 and 6.6 for SI 1/17 and SI 1/20, respectively). Conversely, SI 1/22 resulted more potent towards the HO-2 isoform (HO-1 IC_{50} = 8.95 μM and HO-2 IC_{50} = 1.01 μM).

To check that both SI 1/20 and SI 1/22 can exert inhibitory activity against the target in intact cells, the HO enzymatic activity towards untreated and treated DU145 cells with 10 μM of the tested mutual prodrugs for 72 h was analyzed (Figure 5). Interestingly, both compounds showed a significant reduction of the HO enzymatic activity in cell lysates, likely acting as effective inhibitors *in vitro*. Also, these data further corroborate the feasibility of the mutual prodrugs to release the active parent compounds after effectively crossing the cellular membrane.

Effects of SI 1/20 and SI 1/22 on HO-1 expression and reactive oxygen species (ROS) production levels in DU145 cells

The HO expression levels in DU145 cancer cells after 72 h of treatment with 10 μM of SI 1/20 and SI 1/22, were measured to analyze the possible link between the reduction of cell viability and the modulation of the HO system. As revealed by

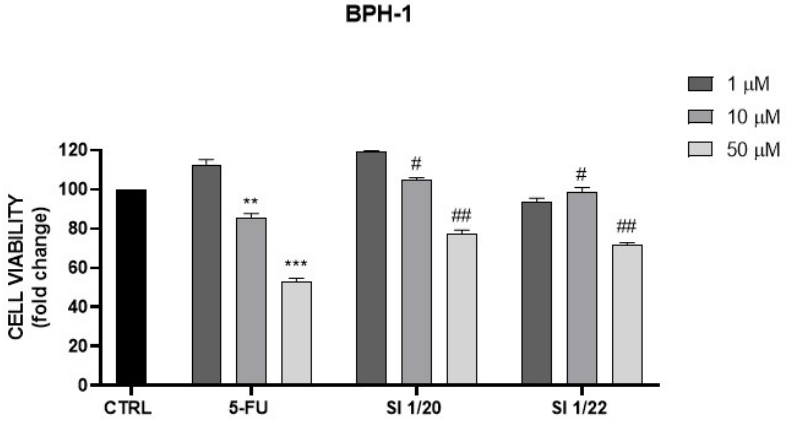

Figure 4. Assessment of 5-FU, SI 1/20 and SI 1/22 effect at 1, 10, 50 μM against BPH-1 cell viability after 72 h treatment. $^{**}p < 0.005$, $^{***}p < 0.0005$ *vs* CTRL; $^{\#}p < 0.05$, $^{\#\#}p < 0.005$ *vs* 5-FU.

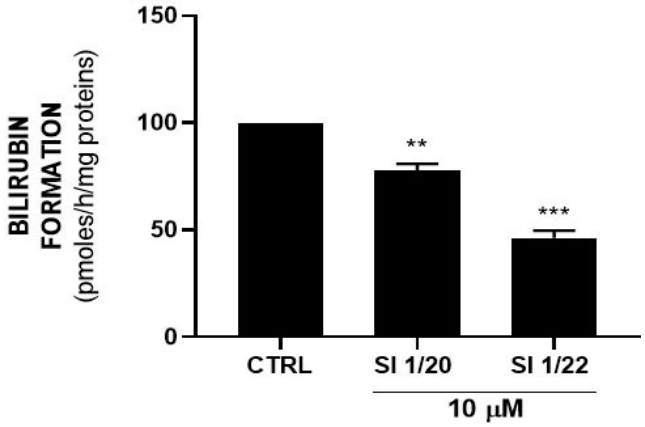

Figure 5. Enzymatic activity in untreated (CTRL) and treated (i.e., SI 1/20 and SI 1/22) DU145 cancer cells. $^{**}p < 0.005$, $^{***}p < 0.0005$ *vs* CTRL.

immunoblots analysis (Figure 6) the new mutual prodrugs markedly affect the HO proteins expression in DU145 cells, with a strong decrease in the HO-1 levels. Surprisingly, 5-FU also reduced the HO-1 levels while no significant change was observed for the HO-2 isoform. According to these results, and in line with the mechanism of action of non-competitive HO-1 inhibitors,[10f,12] SI 1/20 and SI 1/22 can effectively modulate the HO system at two different levels, indeed, via both the pharmacological inhibition and the down-regulation of the target protein.

Finally, since an optimal rate of ROS is required for cancer cell function and proliferation,[28] we hypothesized that a reduction in cell viability might be related to an increase in ROS concentration. Moreover, cell death induction caused by elevated ROS levels has been highlighted as the main mechanism responsible for the effectiveness of monoclonal antibodies, antimetabolites, and tyrosine kinase inhibitors, which represent the core of targeted cancer therapy.[29] Therefore, the ROS levels in DU145 cells after treatment with 5-FU, SI 1/20, and SI 1/22 at three different concentrations (i.e., 1, 10, and 50 μM) and time points (i.e., 1, 3, and 6 h) were measured. Compatible with the negative modulation (i.e., pharmacological inhibition and downregulation) exerted by SI 1/20 and SI 1/22 on the HO system, a significant increase in ROS levels on DU145 cells, in a time- and dose-dependent manner was observed (Figure 7), thus justifying the observed cytotoxic effect in the MTT assay.

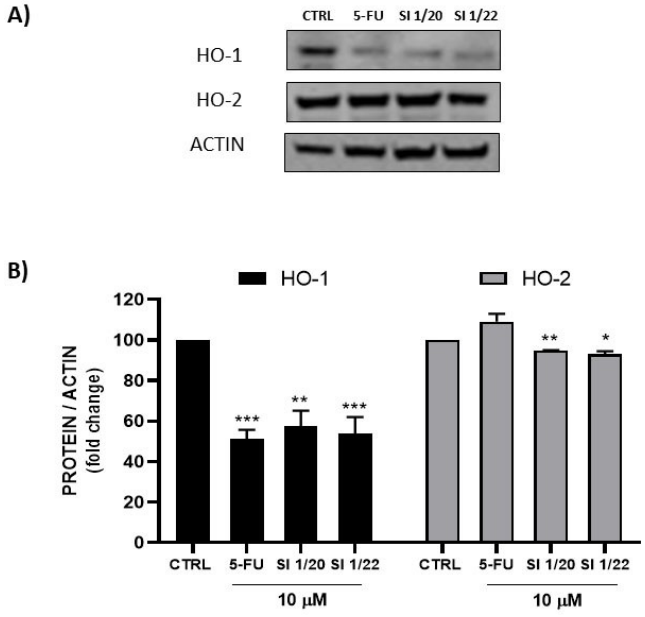

Figure 6. Western blot (**A**) and densitometric (**B**) analysis of the effect of 5-FU, SI 1/20 and SI 1/22 treatment on HO-1 and HO-2 protein levels in DU145 cells. $^{*}p < 0.05$, $^{**}p < 0.005$, $^{***}p < 0.0005$ *vs* untreated control cells (CTRL).

Conclusion

In this work, we reported the discovery of SI 1/20 and SI 1/22 as two novel mutual prodrugs derived from 5-FU and HO-1 inhibitors. The synthesized compounds were obtained using an optimized synthetic method involving the key intermediate 5-FU-succ, providing better yields and simpler purification methods compared to the previously reported one. Obtained results from *in vitro* stability assessment, in aqueous porcine esterase solution and PBS, confirmed that the new mutual prodrugs possessed a suitable hydrolysis rate profile that allows the release of the parent drugs to exert biological activity. In addition, *in silico* ADMET calculations predicted good drug-likeness and pharmacokinetic properties, supporting the possibility of oral administration which is a great advantage with respect to 5-FU. Generally, SI 1/20 and SI 1/22 produced a cytotoxic effect in both tested cancer cell lines similarly or better than 5-FU, and particularly, SI 1/22 was significantly more potent than 5-FU in DU145 prostate cancer cell lines. In addition, both SI 1/20 and SI 1/22 reduced the viability of DU145 cells to a major extent compared to the combination of 5-FU and the corresponding HO-1 inhibitor, thus confirming that a single molecule might use to overcome the disadvantages typically associated with combinational therapy. Remarkably, the new hybrids exhibited significantly lower cytotoxicity compared to 5-FU against non-tumorigenic BPH-1 cells. The observed cytotoxic effects were consistent with the HO enzymatic inhibition in cell lysates, the reduction of the HO-1 expression levels, and the increase of ROS mediated by SI 1/20 and SI 1/22. Altogether these results suggested that combining 5-FU and HO-1 inhibitors to obtain 5-FU/HO-1 inhibitor mutual prodrugs represents a promising strategy for the development of new anticancer agents with some advantages over the reference drug 5-FU. Further studies are needed to extend these findings to other cancer cell lines, as well as to evaluate these molecules in preclinical *in vivo* models. Encapsulation of 5-FU/HO-1 inhibitor hybrids in appropriate nanoparticle systems will be considered in order to avoid an unfavourable early release of parent drugs and drive selective delivery in target cells.

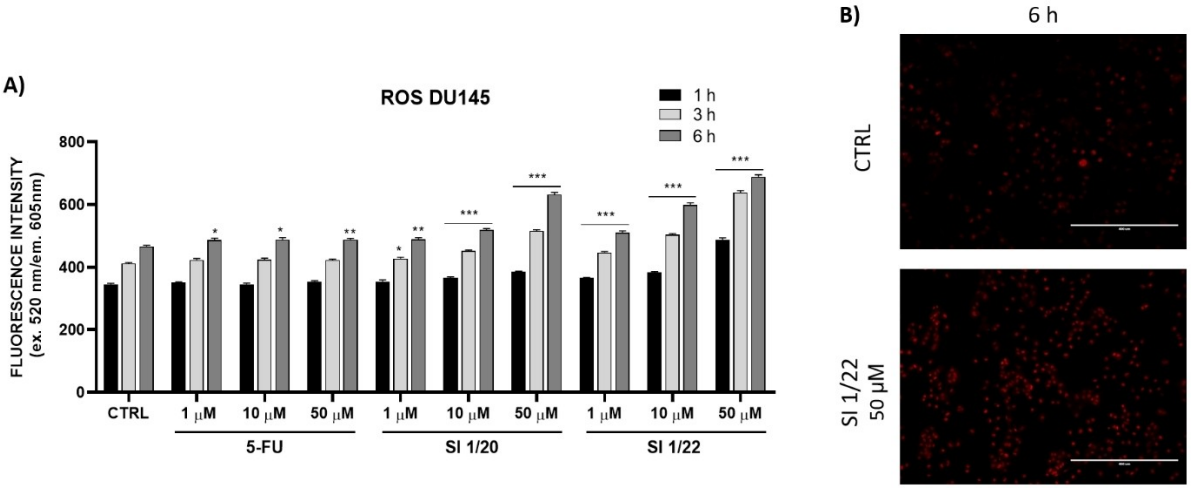

Figure 7. (**A**) Evaluation of ROS levels increase on DU145 cell line after treatment with 5-FU and compounds SI 1/20 and SI 1/22 at different concentrations (1, 10, 50 μM); (**B**) Microscope fluorescence images (scale 400 μm) of the most significant data. *$p < 0.05$, **$p < 0.005$, ***$p < 0.0005$ *vs* CTRL.

Experimental Section

Chemistry

Commercially available reagents and organic solvent were purchased from Sigma-Aldrich or Fluorochem and used without further purification. All reactions were monitored by thin-layer chromatography (TLC), performed on Merck plates (Kieselgel 60 F254), and using UV light ($\lambda = 254$ and 366 nm) and/or iodine staining (iodine chamber) for visualization. Flash column chromatography was performed on glass columns using Merck silica gel 60 0.040–0.063 mm (230–400 mesh) as a stationary phase. Automated flash column chromatography was carried out on a Biotage FlashMaster Personal Plus system with prepacked silica gel columns (Biotage® SNAP cartridge KP-Sil, Uppsala, Sweden). Melting points were determined in an IA9200 Electrothermal apparatus equipped with a digital thermometer in capillary glass tubes and are uncorrected. Infrared spectra were recorded on a Perkin Elmer 281 Fourier-transform infrared (FTIR) spectrometer in KBr disks (KBr, selected lines). Elemental analyses for C, H, N, were within ±0.4% of theoretical values and were performed on a Carlo Erba Elemental Analyser Mod. 1108 apparatus. ^{1}H NMR spectra were acquired on Varian Inova Unity 200 or Varian Inova Unity 500 spectrometers (recorded at 200 and 500 MHz, respectively), while ^{13}C NMR spectra were acquired on Varian Inova Unity 500 (recorded at 126 MHz). Dimethyl sulfoxide-d_6 (DMSO-d_6), containing 0.03% (v/v) tetramethylsilane (TMS) as an internal standard, was used as a deuterated solvent for NMR experiments. Chemical shifts are reported in δ values (ppm), while coupling constants (*J*) are given in Hz. Signal multiplicities are characterized as s (singlet), d (doublet), t (triplet), q (quartet), m (multiplet), br (broad). Mass spectra were recorded on a UPLCMS/MS system consisting of a Waters ACQUITY UPLC (Waters Corporation, Milford, MA, USA) coupled to a Waters TQD mass spectrometer (electrospray ionization mode ESI-tandem quadrupole). Chromatographic separations were carried out using the Acquity UPLC BEH (bridged ethyl hybrid) C18 column; 2.1 mm × 100 mm, and 1.7 μM particle size, equipped with Acquity UPLC BEH C18 Van Guard precolumn; 2.1 mm × 5 mm, and 1.7 μM particle size. The column was maintained at 40 °C and eluted under gradient conditions from 95% to 0% of eluent A over 10 min, at a flow rate of 0.3 mL min^{-1}. Eluent A: water/formic acid (0.1%, v/v), Eluent B: acetonitrile/formic acid (0.1%, v/v). The UPLC/MS purity of final compounds was confirmed to be ≥99%.

4-[(5-Fluoro-2,4-dioxo-1,2,3,4-tetrahydropyrimidin-1-yl)methoxy]-4-oxobutanoic acid (5-FU-succ)

A mixture of 5-FU (1.0 g, 7.68 mmol) in 37% formaldehyde solution (1.38 g, 12.02 mmol) was stirred at 60 °C for 4 h. After that time, the reaction mixture was cooled at room temperature and concentered under vacuum to give a transparent semisolid which was dissolved in dry CH_3CN (10 mL). Subsequently, succinic anhydride (0.98 g, 9.84 mmol) and a catalytic amount of DMAP were added and the mixture thus obtained was heated at 50 °C for 7 h. The precipitate which formed upon cooling was then filtered off, and the organic solvent was removed under reduced pressure to obtain a crude product which was purified using a Biotage® chromatographic system with SNAP KP-Sil flash chromatography cartridges and a mixture of CH_2Cl_2 and CH_3OH (9:1, v/v) as eluent phase. White solid (46%): mp 178.0–179.5 °C; IR (KBr, selected lines): cm^{-1} 3038, 2853, 1754, 1464, 1319, 1261, 1161, 1127, 985, 873; ^{1}H NMR (200 MHz, DMSO-d_6): δ 8.11 (d, $J_{H\text{-}F} = 6.6$ Hz, 1H, CHCF), 5.57 (s, 2H, CH_2O), 2.59–2.38 (m, 2H + 2H, $COCH_2CH_2CO$). Anal. Calcd. for $C_9H_9FN_2O_6$: C, 41.55; H, 3.49; N, 10.77. Found: C, 41.42; H, 3.47; N, 10.79.

General procedure for the synthesis of 5-FU/HO-1 hybrids SI 1/17, SI 1/20, and SI 1/22

To a suspension of the appropriate imidazole-based derivative 1-(3-bromophenyl)-2-(1*H*-imidazol-1-yl)ethanol (S1 1/09), 1-(biphenyl-3-yl)-2-(1*H*-imidazol-1-yl)ethanol (LS 4/28), and 1-{4-[(4-bromobenzyl)oxy]phenyl}-2-(1*H*-imidazol-1-yl)ethanol (LS 6/42) (1.0 equiv) in anhydrous CH_3CN, 5-FU-succ (1.2 equiv), EDC·HCl (1.2 equiv), and DMAP (0.05 equiv) were added. The reaction mixture was stirred at room temperature and under nitrogen flow for 3 h. After this time, the solvent was removed under reduced pressure, and the resulting residue was purified by flash chromatography using a mixture of acetone/petroleum ether (8:2, v/v) as an eluent to afford the following products.

1-[1-(3-Bromophenyl)-2-(1*H*-imidazol-1-yl)ethyl]4-(5-fluoro-2,4-dioxo-1,2,3,4-tetrahydropyrimidin-1-yl)methyl butanediolate (SI 1/17)

The title compound was obtained using 0.152 g (0.57 mmol) of 1-(3-bromophenyl)-2-(1*H*-imidazol-1-yl)ethanol (SI 1/09) in 6 mL of anhydrous CH_3CN, 0.178 g (0.68 mmol) of 5-FU-succ, 0.131 g (0.68 mmol) of EDC·HCl, and a catalytic amount of DMAP. White solid (65 %): UPLC/MS purity 100 %, $t_R = 3.75$ min, $[M+H]^+ = 508.9/510.8$; mp 172.0–174.5 °C; IR (KBr, selected lines): cm^{-1} 3448, 3122, 1732, 1671, 1509, 1412, 1366, 1265, 1171, 1143, 1089, 993; ^{1}H NMR (500 MHz, DMSO-d_6): δ 8.09 (d, $J_{H\text{-}F} = 6.5$ Hz, 1H, CHCF), 7.56 (s, 1H, imidazole), 7.54–7.50 (m, 2H, aromatic), 7.34–7.29 (m, 2H, aromatic), 7.11 (s, 1H, imidazole), 6.85 (s, 1H, imidazole), 5.95 (t, $J = 5.8$ Hz, 1H, O*CH*CH_2), 5.6–5.51 (m, 2H, CH_2O), 4.37 (d, $J = 5.9$ Hz, 2H, OCH*CH*$_2$), 2.69–2.55 (m, 2H + 2H, $COCH_2CH_2CO$); ^{13}C-NMR (126 MHz, DMSO-d_6): δ 171.6, 170.6, 157.4 (d, $J_{C\text{-}F} = 26.5$ Hz), 149.2, 139.7, 139.4 (d, $J_{C\text{-}F} = 230.6$ Hz), 137.8, 131.1, 130.6, 129.4 (d, $J_{C\text{-}F} = 34.0$ Hz), 129.1, 128.2, 125.2, 121.7, 120.0, 73.8, 70.7, 50.1, 28.5, 28.3. Anal. Calcd. for $C_{20}H_{18}BrFN_4O_6$: C, 47.17; H, 3.56; N, 11.00. Found: C, 47.03; H, 3.49; N, 10.95.

1-(1-{[1,1′-Biphenyl]-3-yl}-2-(1*H*-imidazol-1-yl)ethyl)-4-(5-fluoro-2,4-dioxo-1,2,3,4-tetrahydropyrimidin-1-yl)methyl butanedioate (SI 1/20)

The title compound was obtained using 0.127 g (0.48 mmol) of 1-(biphenyl-3-yl)-2-(1*H*-imidazol-1-yl)ethanol (LS 4/28) in 6 mL of anhydrous CH_3CN, 0.150 g (0.58 mmol) of 5-FU-succ, 0.111 g (0.58 mmol) of EDC·HCl, and a catalytic amount of DMAP. White solid (26 %): UPLC/MS purity 100 %, $t_R = 4.46$ min, $[M+H]^+ = 507.3$; mp 119.8–120.7 °C; IR (KBr, selected lines): cm^{-1} 3448, 3067, 1717, 1508, 1458, 1355, 1236, 1133, 1081, 1033, 974, 757, 701; ^{1}H NMR (500 MHz, DMSO-d_6): δ 8.06 (d, $J_{H\text{-}F} = 6.6$ Hz, 1H, CHCF), 7.68–7.28 (m, 9H + 1H, aromatic + imidazole), 7.15 (s, 1H, imidazole), 6.87 (s, 1H, imidazole), 6.03 (t, $J = 5.8$ Hz, 1H, O*CH*CH_2), 5.59–5.50 (m, 2H, CH_2O), 4.48–4.37 (m, 2H, OCH*CH*$_2$), 2.69–2.54 (m, 2H + 2H, $COCH_2CH_2CO$); ^{13}C-NMR (126 MHz, DMSO-d_6): δ 171.7, 170.7, 157.4 (d, $J_{C\text{-}F} = 25.6$ Hz), 149.3, 140.4, 139.8, 139.4 (d, $J_{C\text{-}F} = 230.6$ Hz), 137.9 (C + C), 129.4 (d, $J_{C\text{-}F} = 34.4$ Hz), 129.1, 128.9 (2 C), 127.7, 126.8 (2 C), 126.7, 126.6, 125.2, 124.7, 120.1, 74.6, 70.7, 50.4, 28.5, 28.3. Anal. Calcd. for $C_{26}H_{23}FN_4O_6$: C, 61.66; H, 4.58; N, 11.06. Found: C, 46.92; H, 4.56; N, 11.01.

1-(1-{4-[(4-Bromophenyl)methoxy]phenyl}-2-(1*H*-imidazol-1-yl)ethyl)-4-(5-fluoro-2,4-dioxo-1,2,3,4-tetrahydropyrimidin-1-yl)methyl butanedioate (SI 1/22)

The title compound was obtained using 0.111 g (0.32 mmol) of 1-{4-[(4-bromobenzyl)oxy]phenyl}-2-(1*H*-imidazol-1-yl)ethanol (LS 6/42) in 11 mL of anhydrous CH_3CN, 0.101 g (0.39 mmol) of 5-FU-succ, 0.074 g (0.39 mmol) of EDC·HCl, and a catalytic amount of DMAP. White solid (26 %): UPLC/MS purity 100 %, $t_R = 5.30$ min, $[M+H]^+ = 615.2/617.2$; mp 143.5–144.0 °C; IR (KBr, selected lines): cm^{-1} 3448, 3081, 2960, 1756, 1611, 1513, 1458, 1408, 1357, 1245, 1133, 1001, 832, 754; ^{1}H NMR (500 MHz, DMSO-d_6): δ 8.09 (d, $J_{H\text{-}F} = 6.6$ Hz, 1H, CHCF), 7.61–7.57 (m, 2H, aromatic), 7.50 (s, 1H, imidazole), 7.43–7.39 (m, 2H, aromatic), 7.27–7.23 (m, 2H, aromatic), 7.10 (s, 1H, imidazole), 7.01–6.96 (m, 2H, aromatic), 6.84 (s, 1H, imidazole), 5.92 – 5.88 (m, 1H, O*CH*CH_2), 5.59–5.51 (m, 2H, CH_2O), 5.08 (br, 2H, CH_2O), 4.38–4.28 (m, 2H, OCH*CH*$_2$), 2.58 (br, 2H + 2H, $COCH_2CH_2CO$); ^{13}C-NMR (126 MHz, DMSO-d_6): δ 171.6, 170.6, 158.1, 157.4 (d, $J_{C\text{-}F} = 26.1$ Hz), 149.2, 139.4 (d, $J_{C\text{-}F} = 231.0$ Hz), 137.8, 136.5, 131.4 (2 C), 129.8 (2 C), 129.45 (d, $J_{C\text{-}F} = 34.2$ Hz), 129.40, 128.2, 127.8 (2 C), 120.9, 119.9, 114.7 (2 C), 74.3, 70.6, 68.4, 50.3, 28.5, 28.3. Anal. Calcd. for $C_{27}H_{24}BrFN_4O_7$: C, 52.70; H, 3.93; N, 9.10. Found: C, 52.53; H, 3.92; N, 9.08.

In vitro stability assessment

Hydrolysis stability studies were performed in porcine esterase solution and PBS buffer following a previously reported protocol and using a high-pressure liquid chromatography (HPLC) method for the quantification of the percentage of the compound remaining.[21] HPLC analysis was performed on Shimadzu Prominence-i LC-2030 C 3D Plus equipped with RID20 A, chromatographic separation was carried out using Chromolith SpeedROD RP 18.5 μM, 1.6 × 50 mm, Merck. The pseudo-first-order hydrolysis rate constant (k) and half-life ($t_{1/2}$) were calculated by plotting the natural logarithm (ln) of the area under the curve (AUCt) of the peak at six different time points (0-240 min). Experiments were performed in triplicate.

Biological evaluation

Preparation of spleen and brain microsomal fractions

Rat spleen and brain microsomal fractions were prepared by differential centrifugation to obtain HO-1 and HO-2, respectively. Rat spleen and brain microsomal fractions were selected in order to use the most native (*i.e.*, closest to *in vivo)* forms of HO-1 and HO-2. Spleen and brain (Sprague-Dawley rats) microsomal fractions were prepared according to the procedure outlined by Ryter et al.[30] The experiments reported in the present paper complied with current Italian law and met the guidelines of the Institutional Animal Care and Use Committee of MINISTRY OF HEALTH (Directorate General for Animal Health and Veterinary Medicines) (Italy). The experiments were performed in male Sprague-Dawley albino rats (150 g body weight and age 45 d). Animals had free access to water and were maintained in a temperature- and light-controlled facility. Each rat was sacrificed and their spleen and brain were excised, weighed and pooled to obtain homogenates. Spleen and brain homogenates (15 %, w/v) pooled from four rats was prepared in ice-cold buffer (50 mM Tris buffer, pH 7.4, containing 0.25 M sucrose) using a Potter-Elvehjem homogenizing system with a Teflon pestle. Centrifugation at 10,000 g for 20 min at 4 °C, followed by centrifugation of the supernatant at 100,000 g for 60 min at 4 °C was used to obtain microsomal fractions of rat spleen and brain homogenates. The 100,000 g pellet (microsomes) was resuspended in 100 mM potassium phosphate buffer, pH 7.8, containing 2 mM $MgCl_2$ with a Potter-Elvehjem homogenizing system. Equal aliquots of the rat spleen and brain microsomal fractions were aliquoted and stored at −80 °C for up to 2 months. Protein concentration was measured using TAKE 3 nanodrop.

Preparation of BVR

Liver cytosol has been used as a source of BVR. Rat liver was perfused through the hepatic portal vein with cold 0.9 % NaCl, then it was cut and flushed with 2 x 20 mL of ice-cold PBS to remove all the blood. Liver tissue was homogenized in 3 volumes of a solution containing 1.15 % KCl w/v and Tris buffer 20 mM, pH 7.8 on ice. Homogenates were centrifuged at 10,000 g, for 20 min at 4 °C. The supernatant was decanted and centrifuged at 100,000 g for 1 h at 4 °C to sediment the microsomes. The 100,000 g supernatant was saved and then stored in aliquots at −80 °C after protein concentration was measured.

Cell culture and treatments

Human prostate cancer cells (DU145; ATCC American Type Culture Collection, HTB-81), human lung cancer cells (A549; ATCC American Type Culture Collection, CCL-185-LUC2), and human benign prostatic hyperplasia cells (BPH-1; DSMZ Leibniz Institute DSMZ - German Collection of Microorganisms and Cell Cultures GmbH, ACC 143) were grown in Dulbecco's modified Eagle's medium (DMEM) supplemented with 10% of heat-inactivated fetal bovine serum (FBS), 100 U/ml penicillin and 100 μg/ml streptomycin (Sigma-Aldrich, Steinheim, Germany). Cells were incubated at 37 °C in a humidified atmosphere with 5% CO_2. Cells were seeded into 96-well plates at a density of 7.0 x 10^3 cells/well and after 24 h treated with 5-FU, LS 4/28, LS 6/42, SI 1/20, and SI 1/22 at three different concentrations (1 μM, 10 μM and 50 μM) for 72 h. Furthermore, co-administration of 5-FU and HO-1 inhibitors LS 4/28 and LS 6/42, respectively were tested and compared to the corresponding mutual prodrugs SI 1/20 and SI 1/22, a single concentration was selected (10 μM) and treatment maintained for 72 h.

Measurement of HO enzymatic activity

HO enzymatic activity was tested both in a cell free model and in DU145 cell lysates. As sources of HO-1 and HO-2 isoforms, spleen and brain microsomal fractions were used, respectively as previously reported by Salerno *et al.*[31]

DU145 cells were treated with 5-FU, SI 1/20, and SI 1/22 at the concentration of 10 μM and harvested after 72 h; protein levels in the cell lysates were quantified to evaluate HO enzymatic activity by measuring the BR formation through the difference in absorbance at 464 to 530 nm. Reaction mixtures consisted of 20 mM Tris-HCl (pH 7.4), cell lysate (2 mg/mL), 0.5–2 mg/mL BVR reductase, 1 mM NADPH, 2 mM glucose 6-phosphate (G6P), 1 U G6P dehydrogenase and 25 μM hemin. Incubation was carried out in a circulating water bath in the dark for 1 h at 37 °C. The reaction was stopped by adding chloroform (1:1). After the chloroform phase was recovered, the amount of formed BR was measured with a double-beam spectrophotometer at OD 464–530 nm (extinction coefficient, 40 mM/cm^{-1} for BR). One unit of the enzyme was defined as the amount of enzyme catalyzing the formation of 1 nmol of BR/mg protein/h.

Cell viability assay

In order to evaluate the effect of tested compounds on cell viability, 3-(4,5-dimethylthiazole-2-yl)-2,5-diphenyltetrazolium bromide (MTT) assay was performed. Following the aforementioned treatments, 0.5 mg/ml of MTT (Sigma Aldrich, Steinheim, Germany) was added to each well and incubated for 3 h at 37 °C. Ultimately, 100 μl of DMSO were added to each well to dissolve formazan salts and absorbance was measured at $\lambda = 570$ nm in a microplate reader (Biotek Synergy-HT, Winooski, VT, USA). Eight replicate wells were used for each group and at least three independent experiments were performed.

Western blot analysis

DU145 cells were treated with 5-FU, SI 1/20, SI 1/22 and harvested after 72 h, pellets were sonicated and centrifugated at 2500 rpm for 10 min at 4 °C to extract proteins from the total lysate. Protein samples (70 μg) were diluted in 4× NuPage LDS sample buffer (Invitrogen, Waltham, MA, USA, NP0007), and heated at 80 °C for 5 min. Proteins were separated by electrophoresis and then transferred as previously reported by Sorrenti et al.[32] Membranes were incubated overnight with HO-1 (GTX101147, diluted 1:1000, GeneTex, Irvine, CA, USA), HO-2 (SPA897, diluted 1:2000, Enzo Life Sciences, Farmingdale, New York, USA) and β-actin (GTX109639, diluted 1:7000, GeneTex) primary antibodies. Goat anti-rabbit secondary antibody was used to detect blots (dil. 1:7000). Blots were scanned, and densitometric analysis was performed with the Odyssey Infrared Imaging System (LI–COR, Milan, Italy). Values were normalized to β-actin.

Measurement of ROS

ROS levels were determined in live cells (DU145) using the Cellular Reactive Oxygen Species Detection Assay Kit (ab186027, Abcam, Cambridge, UK). Briefly, cells were seeded in a black 96-well plate at a density of 1.0 x 10^4 cells/well and stained with ROS red working solution following the manufacturer's instructions. After 1 h of incubation (37 °C, 5% CO_2) with the staining solution cells were treated with 5-FU, SI 1/20, SI 1/22, and changes in fluorescence intensity were monitored by time course-reading (1-3-6 h) in a microplate reader (Ex/Em = 520/605 nm). Pictures were taken after 6 h of treatment highlight a significant difference between the control group and the SI 1/22 treated group. Eight replicate wells were used for each group.

Statistical analysis

At least three independent experiments were performed for each analysis. The statistical significance ($p < 0.05$) of the differences between the experimental groups was determined by Fisher's method for analysis of multiple comparisons. For comparison between treatment groups, the null hypothesis was tested by either a single-factor analysis of variance (ANOVA) for multiple groups or an unpaired t-test for two groups, data are presented as mean ± SEM.

Acknowledgements

This work was financially supported by a grant from the University of Catania, Programma Ricerca di Ateneo Pia.Ce.Ri 2020–2022 Linea 3 Starting Grant, POLYPHARMA-CT, project code: 57722172141 to S.I.; V.S. was supported by project authorized by the Ministry of Health (Directorate General for Animal Health and Veterinary Medicines) "Dosing of enzymatic activities in rat microsomes" 2018–2022, project code: 02769.N.VLY; V.P. was supported by the University of Catania, Programma Ricerca di Ateneo Pia.Ce.Ri 2020–2022 linea 2, project code: 57722172126. S.I. thanks for the support of the PON R&I funds 2014–2020 (E66 C18001320007, AIM1872330, activity 1). The authors thank Dr. Vittorio Canale (Jagiellonian University Medical College) for his assistance in HPLC analysis. Open Access funding provided by Università degli Studi di Catania within the CRUI-CARE Agreement.

Conflict of Interest

The authors declare no conflict of interest.

Data Availability Statement

The data that support the findings of this study are available in the supplementary material of this article.

Keywords: Prodrugs · cancer · 5-fluorouracil · heme oxygenase 1 · DU145 prostate cancer cells

[1] J. Ferlay, M. Ervik, F. Lam, M. Colombet, L. Mery, M. Piñeros, A. Znaor, I. Soerjomataram, F. Bray, Available from: https://gco.iarc.fr/today, accessed 08 March 2022 **2020**.
[2] H. Sung, J. Ferlay, R. L. Siegel, M. Laversanne, I. Soerjomataram, A. Jemal, F. Bray, *Ca-Cancer J. Clin.* **2021**, *71*, 209–249.
[3] R. Moynihan, S. Sanders, Z. A. Michaleff, A. M. Scott, J. Clark, E. J. To, M. Jones, E. Kitchener, M. Fox, M. Johansson, E. Lang, A. Duggan, I. Scott, L. Albarqouni, *BMJ Open* **2021**, *11*, e045343.
[4] R. Edge, J. Meyers, G. Tiernan, Z. Li, A. Schiavuzzi, P. Chan, A. Vassallo, A. Morrow, C. Mazariego, C. E. Wakefield, K. Canfell, N. Taylor, *PLoS One* **2021**, *16*, e0257420.
[5] Q. Li, L. C. Hwang, *Cancer Med.* **2020**, *9*, 6079–6081.
[6] a) N. G. Abraham, A. Kappas, *Pharmacol. Rev.* **2008**, *60*, 79–127; b) S. Intagliata, L. Salerno, V. Ciaffaglione, C. Leonardi, A. N. Fallica, G. Carota, E. Amata, A. Marrazzo, V. Pittala, G. Romeo, *Eur. J. Med. Chem.* **2019**, *183*, 111703.
[7] L. L. Dunn, R. G. Midwinter, J. Ni, H. A. Hamid, C. R. Parish, R. Stocker, *Antioxid. Redox Signal.* **2014**, *20*, 1723–1742.
[8] M. D. Maines, *Curr. Protoc. Toxicol.* **2001**, *Chapter 9*, Unit 9 1.
[9] S. M. Keyse, R. M. Tyrrell, *Proc. Natl. Acad. Sci. USA* **1989**, *86*, 99–103.
[10] a) G. Romeo, V. Ciaffaglione, E. Amata, M. Dichiara, L. Calabrese, L. Vanella, V. Sorrenti, S. Grosso, A. G. D'Amico, V. D'Agata, S. Intagliata, L. Salerno, *Molecules* **2021**, *26*, 3860; b) K. C. Chiang, K. H. Tsui, Y. H. Lin, C. P. Hou, K. S. Chang, H. H. Tsai, Y. S. Shin, C. C. Chen, T. H. Feng, H. H. Juang, *Transl. Oncol.* **2020**, *13*, 102–112; c) S. Jana, K. Patra, J. Jana, D. P. Mandal, S. Bhattacharjee, *Chem.-Biol. Interact.* **2018**, *285*, 59–68; d) P. Liu, D. Ma, Z. Yu, N. Zhe, M. Ren, P. Wang, M. Yu, J. Huang, Q. Fang, J. Wang, *Biomed. Pharmacother.* **2017**, *91*, 21–30; e) A. Jozkowicz, H. Was, J. Dulak, *Antioxid. Redox Signal.* **2007**, *9*, 2099–2117; f) A. N. Fallica, V. Sorrenti, A. G. D'Amico, L. Salerno, G. Romeo, S. Intagliata, V. Consoli, G. Floresta, A. Rescifina, V. D'Agata, L. Vanella, V. Pittalà, *J. Med. Chem.* **2021**, *64*, 13373–13393.
[11] M. Nitti, S. Piras, U. M. Marinari, L. Moretta, M. A. Pronzato, A. L. Furfaro, *Antioxidants (Basel)* **2017**, *6*, 29.
[12] P. Podkalicka, O. Mucha, A. Józkowicz, J. Dulak, A. Łoboda, *Contemp. Oncol. (Pozn).* **2018**, *22*, 23–32.
[13] D. B. Longley, D. P. Harkin, P. G. Johnston, *Nat. Rev. Cancer* **2003**, *3*, 330–338.
[14] a) C. Manogue, P. Cotogno, M. M. Moses, P. C. Barata, J. L. Layton, A. O. Sartor, B. E. Lewis, *J. Clin. Oncol.* **2019**, *37*, 319–319; b) T. Ibrahim, A. Di Paolo, F. Amatori, L. Mercatali, E. Ravaioli, E. Flamini, E. Sacanna, M. Del Tacca, R. Danesi, D. Amadori, *J. Clin. Pharmacol.* **2012**, *52*, 361–369.
[15] a) J. S. Macdonald, *Oncology (Williston Park)* **1999**, *13*, 33–134; b) G. Milano, A. L. Chamorey, *Chronobiol. Int.* **2002**, *19*, 177–189.
[16] a) M. Malet-Martino, P. Jolimaitre, R. Martino, *Curr. Med. Chem. Anti-Cancer Agents* **2002**, *2*, 267–1310; b) M. Malet-Martino, R. Martino, *Oncologist* **2002**, *7*, 288–323.
[17] V. Ciaffaglione, M. N. Modica, V. Pittalà, G. Romeo, L. Salerno, S. Intagliata, *ChemMedChem* **2021**, *16*, 3496–3512.
[18] Y. Jiang, X. Li, J. Hou, Y. Huang, Y. Jia, M. Zou, J. Zhang, X. Wang, W. Xu, Y. Zhang, *Eur. J. Med. Chem.* **2016**, *121*, 649–657.
[19] R. Zhang, X.-Q. Song, R.-P. Liu, Z.-Y. Ma, J.-Y. Xu, *J. Med. Chem.* **2019**, *62*, 4543–4554.
[20] a) F. M. Menger, M. J. Rourk, *J. Org. Chem.* **1997**, *62*, 9083–19088; b) H. E. Taylor, K. B. Sloan, *J. Pharm. Sci.* **1998**, *87*, 15–20.
[21] L. Salerno, L. Vanella, V. Sorrenti, V. Consoli, V. Ciaffaglione, A. N. Fallica, V. Canale, P. Zajdel, R. Pignatello, S. Intagliata, *J. Enzyme Inhib. Med. Chem.* **2021**, *36*, 1378–1386.
[22] L. Salerno, E. Amata, G. Romeo, A. Marrazzo, O. Prezzavento, G. Floresta, V. Sorrenti, I. Barbagallo, A. Rescifina, V. Pittalà, *Eur. J. Med. Chem.* **2018**, *148*, 54–62.
[23] T. Sander, J. Freyss, M. von Korff, C. Rufener, *J. Chem. Inf. Model.* **2015**, *55*, 460–473.
[24] S. K. Lee, I. H. Lee, H. J. Kim, G. S. Chang, J. E. Chung, K. T. No, *in EuroQSAR 2002 Designing Drugs and Crop Protectants: Processes, Problems and Solutions (Blackwell Publishing)* **2003**, 418–420.
[25] C. A. Lipinski, F. Lombardo, B. W. Dominy, P. J. Feeney, *Adv. Drug Delivery Rev.* **2001**, *46*, 3–26.
[26] T. I. Oprea, *J. Comput.-Aided Mol. Des.* **2000**, *14*, 251–264.
[27] a) G. Floresta, A. Carotti, F. Ianni, V. Sorrenti, S. Intagliata, A. Rescifina, L. Salerno, A. Di Michele, R. Sardella, V. Pittalà, *Bioorg. Chem.* **2020**, *99*, 103777; b) V. Ciaffaglione, S. Intagliata, V. Pittalà, A. Marrazzo, V. Sorrenti, L. Vanella, A. Rescifina, G. Floresta, A. Sultan, K. Greish, L. Salerno, *Int. J. Mol. Sci.* **2020**, *21*, 1923.
[28] G. Y. Liou, P. Storz, *Free Radical Res.* **2010**, *44*, 479–496.
[29] B. Perillo, M. Di Donato, A. Pezone, E. Di Zazzo, P. Giovannelli, G. Galasso, G. Castoria, A. Migliaccio, *Exp. Mol. Med.* **2020**, *52*, 192–203.
[30] S. W. Ryter, J. Alam, A. M. Choi, *Physiol. Rev.* **2006**, *86*, 583–650.
[31] L. Salerno, V. Pittalà, G. Romeo, M. N. Modica, A. Marrazzo, M. A. Siracusa, V. Sorrenti, C. Di Giacomo, L. Vanella, N. N. Parayath, K. Greish, *Eur. J. Med. Chem.* **2015**, *96*, 162–172.
[32] V. Sorrenti, A. G. D'Amico, I. Barbagallo, V. Consoli, S. Grosso, L. Vanella, *Biomol. Eng.* **2021**, *11*, 917.

Manuscript received: January 28, 2023
Accepted manuscript online: February 9, 2023
Version of record online: ■■, ■■

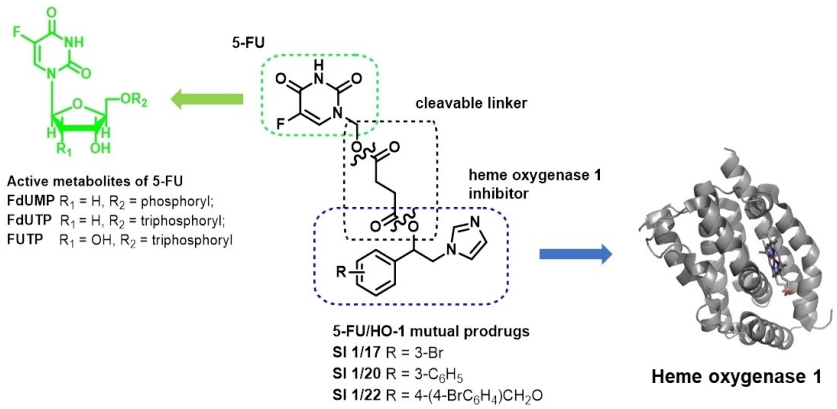

*L. Salerno, V. Sorrenti, V. Pittalà, V. Consoli, M. N. Modica, G. Romeo, A. Marrazzo, M. Giuliano, P. Zajdel, L. Vanella, S. Intagliata**

1 – 12

Discovery of SI 1/20 and SI 1/22 as Mutual Prodrugs of 5-Fluorouracil and Imidazole-Based Heme Oxygenase 1 Inhibitor with Improved Cytotoxicity in DU145 Prostate Cancer Cells

Heme oxygenase 1 (HO-1) is an enzyme that is overexpressed in many cancers, contributing to their spread and invasiveness; therefore, HO-1 inhibition is a promising approach in cancer chemotherapy. 5-Fluorouracil (5-FU) is a well-known antimetabolite drug used as a first-line antineoplastic agent in the treatment of several tumors, yet its therapeutic efficacy is mitigated by low druglike properties and severe side effects. In this study, 5-FU-based mutual prodrugs with promising *in vitro* anticancer activity were developed.